Nonlinear Analysis: Modelling and Control, Vol. 30, No. 2, 252–269
https://doi.org/10.15388/namc.2025.30.38965

Vilnius University Press

Notes on the losses compensation of a three-phase power system with DC offset based on geometric algebras*

Johanka Brdečková, Jaroslav Hrdina

Institute of Mathematics, Faculty of Mechanical Engineering,
Brno University of Technology,
Technická 2896/2, 616 69 Brno, Czech Republic
171519@vutbr.cz; qmhrdina@vutbr.cz

Received: April 25, 2024 / **Revised:** January 24, 2025 / **Published online:** February 26, 2025

Abstract. In a three-phase symmetric power system, we propose a transformation that converts the original current to a current with minimal losses while preserving the standard constraints. The selected transformation is realized in suitable geometric algebra and is not time-dependent. The proposed transformation uses the group symmetry of conformal geometric algebra, mainly rotations and tations.

Keywords: geometric algebra, PGA, CGA, three-phase systems.

1 Introduction

Geometric algebras (GA) represent an object-oriented approach allowing to replace the matrix formalism by a linear notation [13, 16]. In the last years, there has been a rapid development of their use in different areas [1, 8, 9, 17]. Currently, a wide range of other applications are becoming available, in addition to classical applications such as robotics [7, 11], computer graphics [4] or binocular vision [10].

In context of power systems, the concept of GA allows us to express electromagnetic Maxwell's equations uniformly instead of using variable tools like complex numbers, matrices, etc. [15]. In particular, we deal with the three-phase or, generally, n-phase circuit with voltages $v_1, \dots v_n$ and currents $i_1, \dots, i_n$ at the branches. In this context, we can see voltage (resp. current) as vectors $\boldsymbol{v} = v_1 e_1 + \dots + v_n e_n$ (resp. $\boldsymbol{i}_{\mathrm{orig}} = i_1 e_1 + \dots + i_n e_n$) in n-dimensional Euclidean space.

With the help of the Clark transformation, the balanced three-phase circuit can be expressed by only two coordinates because the current lies on a plane that goes through the origin and is perpendicular to the vector $(1, 1, 1)$. In the text, this plane will be denoted as ρ_0. The papers [5, 14] show how Clark transformation can be done by rotating plane ρ_0 to the plane xy. Note that even though we are dealing with a three-phase power system,

*Supported by the grant No. FSI-S-23-8161.

the GA are dimensional independent, and our apparatus can be applied to general n-phase power systems.

Our paper deals with symmetric balanced power systems (Section 5) and with power systems with DC offset (Section 6). In addition, the results of Section 4 are formulated for any systems in a specific time.

In the text, we consider the given voltage $\boldsymbol{v} = v_a e_1 + v_b e_2 + v_c e_3$ and current $\boldsymbol{i}_{\mathrm{orig}} = i_a e_1 + i_b e_2 + i_c e_3$. The scalar part of the power is given by the inner product $p = \boldsymbol{v} \cdot \boldsymbol{i}_{\mathrm{orig}}$ (whole power contains also the bivector part $\boldsymbol{v} \wedge \boldsymbol{i}_{\mathrm{orig}}$). We aim to find a current $\boldsymbol{i}$ to preserve the power while minimizing losses. Then we find a transformation that transforms the original current $\boldsymbol{i}_{\mathrm{orig}}$ to the calculated one $\boldsymbol{i}$, and its trajectories are the shortest ones [2, 18].

We differ from the classical papers, like [14], in the choice of the particular GA. The vector geometric algebra $\mathbb{G}_n$, which is usually used, can represent rotations (or, more precisely, reflections with respect to planes passing through the origin). At distinct from that, in projective geometric algebra (PGA), we can represent all the linear transformations and objects, which enables us to find a plane τ of feasible currents. We will represent voltages (resp. currents) by points with corresponding positional vectors. In PGA, we can easily project points onto planes, while we still benefit from everything from group of rotations.

Finally, to find the optimal transformation in the case of a periodic signal, it is beneficial to use the dilation, so it is a natural to use conformal geometric algebra (CGA). We extend the workspace by an additional dimension to find the expected transformation. Simultaneously, in the text, we demonstrate our approach through the specific examples.

2 Geometric algebras (GA)

The simplest geometric algebra (GA) is a Clifford algebra $\mathcal{C}l(n, 0, 0)$, i.e., Clifford algebra generated by a vector space $\mathbb{R}^n$ equipped with a positive definite quadratic form [13, 16]. This GA is called the vector geometric algebra (VGA) and denoted $\mathbb{G}_n$. The main operation is the geometric product, which is anticommutative on vectors, i.e.,

$$e_i e_j = \begin{cases} -e_j e_i & \text{if } i \neq j \\ 1 & \text{if } i = j = 1, 2, \dots, n, \end{cases}$$

associative, and distributive. Another important operations are the wedge product $\wedge$ and the inner product $\cdot$ defined as projections of geometric product to maximal and zero gradation.

The space of bivectors (second-grade elements) of this algebra forms the Lie algebra isomorphic to the Lie algebra $\mathfrak{so}(n)$ and the associated Lie group to the Lie group $\mathrm{Spin}(n)$. In the case of $n = 3$, to the Lie algebra $\mathfrak{so}(3)$ and a Lie group of unit quaternions.

2.1 Conformal geometric algebra (CGA)

By adding Witt pair $\{e_0, e_\infty\}$ to the VGA $\mathbb{G}_n$ we get an n-dimensional conformal geometric algebra (nCGA) [4, 6]. By Witt pair we mean a pair of generators $\{e_0, e_\infty\}$, which are orthogonal to the original ones and satisfies identities $e_0^2 = e_\infty^2 = 0$ and $e_0 \cdot e_\infty = -1$ [13]. We receive an Clifford algebra $\mathcal{C}l(n+1,1)$ through this procedure, and the inclusion $\iota : \mathbb{R}^n \to \mathcal{C}l(n+1,1)$ is a map

$$\iota(x_1,\dots,x_n) = e_0 + x_1e_1 + \cdots + x_ne_n + \frac{1}{2}\left(x_1^2 + \cdots + x_n^2\right)e_\infty.$$

Using nCGA, we can represent affine geometric objects $O \subset \mathbb{R}^n$. With the help of the inner and outer product, we can define two representations, direct and dual, in the following:

$$\begin{aligned} x \in O \quad &\Longleftrightarrow \quad x \cdot O = 0, \\ x \in O \quad &\Longleftrightarrow \quad (x \cdot O)^* = x \wedge O^* = 0, \end{aligned} \tag{1}$$

respectively, where the duality is assigned by * and means that $A^* = AI$, where I is pseudoscalar $I = e_{1\dots n0\infty} = e_1 \wedge \cdots \wedge e_n \wedge e_0 \wedge e_\infty$. Clearly, the objects from (1) are represented by projective classes in this algebra, which means that for all $\lambda \neq 0 \in \mathbb{R}$, λA represents the same entity. Finally, to join points $A = \iota(x_1,\dots,x_n)$ and $B = \iota(x_1,\dots,x_n)$, the operation join $\vee$ is used:

$$A \vee B = (A^* \wedge B^*)^*.$$

In the case of three-phase power systems, we will work in the algebra 3CGA. In case $n = 3$, we are talking simply about conformal geometric algebra (CGA), and the inclusion $\iota : \mathbb{R}^3 \to \mathcal{C}l(4,1)$ is a map

$$\iota(x,y,z) = e_0 + xe_1 + ye_2 + ze_3 + \frac{1}{2}\left(x^2 + y^2 + z^2\right)e_\infty.$$

Table 1 gives us an overview of geometric objects that can be represented in CGA. In the case of CGA, the bivectors form a conformal Lie algebra $\mathfrak{co}(3)$ and hence an affine Lie algebra $\mathfrak{aff}(3)$ as its subalgebra. The corresponding rotations are in the form of

$$\mathcal{R} = \exp\left(-\frac{\theta}{2}(n_1e_{23} + n_2e_{31} + n_3e_{12})\right),$$

where $n_1e_{23} + n_2e_{31} + n_3e_{12}$ is a rotation plane, and θ is an angle of rotation. Finally, translations are in the form

$$\mathcal{T} = \exp\left(-\frac{1}{2}(t_1e_{1\infty} + t_2e_{2\infty} + t_3e_{3\infty})\right),$$

where $t_1e_1 + t_2e_2 + t_3e_3$ is direction of translation.

Remark. Let us note that some previous considerations are determined by choosing a particular geometric algebra and are not general rules. If $n \geqslant 2$, then all elements of $\mathrm{Spin}(n)$ are exponentials of bivectors. This does not apply to every spin group. For example, the group $\mathrm{Spin}_+(1,3) \cong SL(2,\mathbb{C})$ contains elements that are not exponentials of bivectors [13].

Table 1. Geometric objects in PGA and CGA.

	PGA		CGA	
	direct	dual	direct	dual
line	$(A \vee B)^{*_1}$	$A \vee B$	$(A \wedge B \wedge e_\infty)^{*_2}$	$A \wedge B \wedge e_\infty$
circle			$(A \wedge B \wedge C)^{*_2}$	$A \wedge B \wedge C$
plane	$(A \vee B \vee C)^{*_1}$	$A \vee B \vee C$	$(A \wedge B \wedge C \wedge e_\infty)^{*_2}$	$A \wedge B \wedge C \wedge e_\infty$
sphere			$(A \wedge B \wedge C \wedge D)^{*_2}$	$A \wedge B \wedge C \wedge D$
Here $A^{*_1} = \sharp(A^*)$ and $A^{*_2} = Ae_{1230\infty}$.				

2.2 Projective geometric algebra (PGA)

We get projective geometric algebra (PGA) by taking only linear objects in the dual version of CGA [3,12]. In particular, in CGA, we consider so called flat points $\iota(x_1, x_2, x_3) \wedge e_\infty$, its dual and rename e_∞ to e_0 (this is only because, in PGA theory, the label e_0 for the additional element has been originally introduced). Formally, we use the mapping $\sharp : CGA \to CGA$, which leaves e_i, $i \in \{1,2,3\}$ on place and overwrites $e_0 \to e_\infty$ and $e_\infty \to e_0$ [12]. We demonstrate this correspondence in more detail by the following calculation:

$$\begin{aligned}
&\sharp\big((\iota(x,y,z) \wedge e_\infty)^*\big) \\
&\quad = \sharp\big((e_0 \wedge e_\infty + xe_1 \wedge e_\infty + ye_2 \wedge e_\infty + ze_3 \wedge e_\infty)^*\big) \\
&\quad = \sharp((1 + e_0e_\infty + xe_1e_\infty + ye_2e_\infty + ze_3e_\infty)e_{123}(-1 - e_\infty e_0)) \\
&\quad = -\sharp\big((1 + e_0e_\infty + xe_1e_\infty + ye_2e_\infty + ze_3e_\infty)e_{123} + e_{123}(e_\infty e_0)\big) \\
&\quad = -\sharp\big(1 + (e_0e_\infty + e_\infty e_0) + xe_1e_\infty + ye_2e_\infty + ze_3e_\infty\big)e_{123} \\
&\quad = -\sharp(1 - 2 + xe_1e_\infty + ye_2e_\infty + ze_3e_\infty)e_{123} \\
&\quad = -\sharp(-e_{123} - xe_1e_{123}e_\infty - ye_2e_{123}e_\infty - ze_3e_{123}e_\infty) \\
&\quad = \sharp(e_{123} + xe_{23}e_\infty - ye_{13}e_\infty + ze_{12}e_\infty) \\
&\quad = e_{123} + xe_{023} - ye_{013} + ze_{012}.
\end{aligned}$$

The vectors $\{e_1, e_2, e_3, e_0\}$ forms a Clifford algebra $\mathcal{C}l(3,0,1)$ based on the quadratic form of degenerate signature $(3,0,1)$. The bivectors of this algebra correspond directly to the affine Lie algebra $\mathfrak{aff}(3)$, and its exponents to the spin affine group, which can be seen as a semidirect product $\mathrm{Spin}(3) \rtimes \mathbb{R}^3$. The origin is represented by the blade $o = e_1 \wedge e_2 \wedge e_3$, and the inclusion of $\mathbb{R}^3$ by the map

$$\iota(x,y,z) = e_1 \wedge e_2 \wedge e_3 + xe_0 \wedge e_2 \wedge e_3 + ye_1 \wedge e_0 \wedge e_3 + ze_1 \wedge e_2 \wedge e_0. \tag{2}$$

Note that we can see linear objects in CGA as objects in PGA and define a reduction of the map $A \mapsto \sharp(A^*)$ to PGA $\subset$ CGA, we receive a PGA duality $A \mapsto A^*$.

In this notation, we can see vectors $\boldsymbol{x} = xe_1 + ye_2 + ze_3$ from $\mathbb{G}_3$ as free vectors x^* in PGA and the PGA inclusion (2) of the point X with positional vector $\boldsymbol{x} \in \mathbb{R}^n$ as

$$X = (\boldsymbol{x} + e_0)^* = \iota(x,y,z).$$

Table 1 gives us an overview of geometric objects that can be represented in PGA. For example, in direct representation, the hyperplane π given by equation $\boldsymbol{n} \cdot \boldsymbol{x} = d$, where $\boldsymbol{n} \in \mathbb{R}^n$ has representation

$$\pi = \boldsymbol{n} + de_0, \tag{3}$$

and the linear object given as the intersection of hyperplanes π and σ is given by $\pi \wedge \sigma$. In PGA, it is convenient to use orthogonal projections, we get the projection Y of a point X onto an object l

$$Y = (l \cdot X) \wedge l,$$

where $l \cdot X$ represents the object passing through X perpendicular to l.

3 Three phase power systems with and without DC offset

Consider a symmetric three-phase power supply system with DC offset, i.e., three conductors each carry an alternating current of the same frequency and voltage amplitude such that the power system can be described using periodic functions as

$$\begin{aligned} v_a(t) &= V_n + \sqrt{2}V_{\max}\cos(\omega t), & i_a(t) &= I_n + \sqrt{2}I_{\max}\cos(\omega t + \varphi), \\ v_b(t) &= V_n + \sqrt{2}V_{\max}\cos\left(\omega t + \frac{2}{3}\pi\right), & i_b(t) &= I_n + \sqrt{2}I_{\max}\cos\left(\omega t + \frac{2}{3}\pi + \varphi\right), \\ v_c(t) &= V_n + \sqrt{2}V_{\max}\cos\left(\omega t - \frac{2}{3}\pi\right), & i_c(t) &= I_n + \sqrt{2}I_{\max}\cos\left(\omega t - \frac{2}{3}\pi + \varphi\right). \end{aligned} \tag{4}$$

A phase difference is, in this case, one third of a cycle, but thanks to the nonzero offset, it does not lie in the plane passing through the origin; see Fig. 1 for the three-phased power system with DC offset.

As we mentioned before, in the phase space, we can understand expression (4) as a circle in $\mathbb{R}^3$, where centers of such a parametrized circles are $S_V = [V_n, V_n, V_n]$ and $S_I = [I_n, I_n, I_n]$, respectively. In Figs. 1 and 2 you can see that in the case of a zero offset, i.e., $V_n = I_n = 0$, the circle passes through the origin (see Fig. 2(b)), and in the case of a nonzero offset, the circuit is centered outside the origin (see Fig. 1(b)). On the other hand, both circles have the same normal vector.

Finally, remark that a periodic signal in the symmetric and balanced form without offset has the following description:

$$\begin{aligned} v_a(t) &= \sqrt{2}V_{\max}\cos(\omega t), & i_a(t) &= \sqrt{2}I_{\max}\cos(\omega t + \varphi), \\ v_b(t) &= \sqrt{2}V_{\max}\cos\left(\omega t + \frac{2}{3}\pi\right), & i_b(t) &= \sqrt{2}I_{\max}\cos\left(\omega t + \frac{2}{3}\pi + \varphi\right), \\ v_c(t) &= \sqrt{2}V_{\max}\cos\left(\omega t - \frac{2}{3}\pi\right), & i_c(t) &= \sqrt{2}I_{\max}\cos\left(\omega t - \frac{2}{3}\pi + \varphi\right). \end{aligned} \tag{5}$$

In order to be able to work with the geometric interpretation of signals (and use GA apparatus) in the following sections, let us summarize some basic facts.

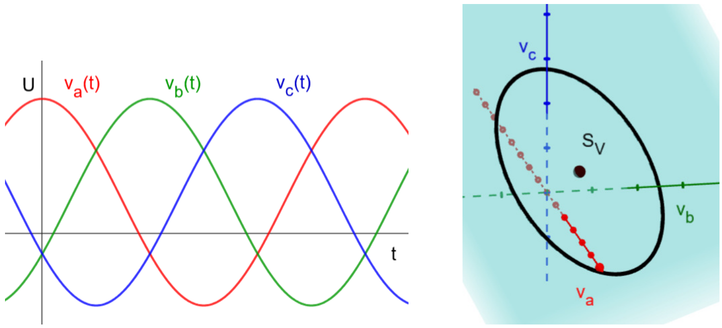

(a) Normalized waveforms (b) Normalised phase space

Figure 1. Three-phased power system with DC offset.

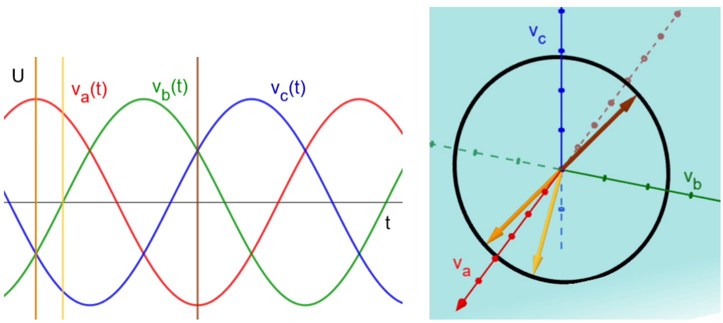

(a) Normalized waveforms (b) Normalised phase space

Figure 2. Balanced three-phased power system.

Lemma 1. *Let us have symmetric power system based on Eqs.* (4)*. Then the scalar part of the electric power* $p = \boldsymbol{v} \cdot \boldsymbol{i}_{\mathrm{orig}}$ *is constant* (*does not depend on* t)*, and*

$$p = 3\bigl(V_n I_n + V_{\max} I_{\max} \cos(\varphi)\bigr).$$

Proof. The straightforward computation

$$p = \boldsymbol{v} \cdot \boldsymbol{i}_{\mathrm{orig}} = 3V_n I_n + 3V_{\max} I_{\max} \cos(\varphi)$$

complete the proof. □

Corollary 1. *Let us have symmetric power system without offset, i.e., system based on Eqs.* (5)*. Then the scalar part of the electric power* $p = \boldsymbol{v} \cdot \boldsymbol{i}_{\mathrm{orig}}$ *is constant and is the following*:

$$p = 3V_{\max} I_{\max} \cos(\varphi).$$

Lemma 2. *The trajectory of voltage* $v \in \mathbb{R}^3$ (5) *is the circle in the plane* $\rho_0 = e_1 + e_2 + e_3$*; see* (3)*. The center is at the origin, and the radius is* $r = \sqrt{3} V_{\max}$.

Proof. The trajectory of voltage $v \in \mathbb{R}^3$ (5) is the circle in the plane ρ_0 because the sum of voltage coordinates is equal to zero for all $t \in \langle 0, \infty)$:

$$\sqrt{2}V_{\max}\cos(t) + \sqrt{2}V_{\max}\cos\left(\omega t + \frac{2\pi}{3}\right) + \sqrt{2}V_{\max}\cos\left(\omega t - \frac{2\pi}{3}\right) = 0.$$

The fact that the centre is origin is clearly seen from parametrization (5), and the radius is determined by the following straightforward calculation, where we denote $c_\alpha = \cos(\alpha)$ and $s_\alpha = \sin(\alpha)$:

$$\begin{aligned}
r &= \sqrt{2V_{\max}^2\bigl(c_{\omega t}^2 + c_{(\omega t+\frac{2\pi}{3})}^2 + c_{(\omega t-2\pi/3)}^2\bigr)} \\
&= \sqrt{2}\,V_{\max}\sqrt{c_{\omega t}^2 + (c_{\omega t}c_{(2\pi/3)} - s_{\omega t}s_{(2\pi/3)})^2 + (c_{\omega t}c_{(-2\pi/3)} - s_{\omega t}s_{t(-2\pi/3)})^2} \\
&= \sqrt{2}\,V_{\max}\sqrt{c_{\omega t}^2 + 2c_{\omega t}^2\left(-\frac{1}{2}\right)^2 + 2s_{\omega t}^2\left(\frac{\sqrt{3}}{2}\right)^2} = \sqrt{2}\,V_{\max}\left(\frac{3}{2}\bigl(c_{\omega t}^2 + s_{\omega t}^2\bigr)\right)^{0.5} \\
&= \sqrt{2}\,V_{\max}\sqrt{\frac{3}{2}} = \sqrt{3}\,V_{\max},
\end{aligned}$$

which completes the proof. □

4 Current of power systems at a specific time

Consider a three-phases current and a three-phases voltage (4) in a specific time t_0 and so omit the time parameter t. In a specific time, a current and a voltage can be represented as concrete vectors in $\mathbb{G}_3$, i.e.,

$$\boldsymbol{i}_{\mathrm{orig}} = i_a e_1 + i_b e_2 + i_c e_3, \qquad \boldsymbol{v} = v_a e_1 + v_b e_2 + v_c e_3,$$

respectively. Now, we express the real part of the power of the system as $p = \boldsymbol{v} \cdot \boldsymbol{i}_{\mathrm{orig}}$ in a time t_0 with the help of the inner product. The aim is to find a new vector $\boldsymbol{i}$ such that the real part of the power

$$p = \boldsymbol{v} \cdot \boldsymbol{i} \tag{6}$$

is preserved, and at the same time, the losses of the system are minimal, where the losses are functions defined as follows:

$$\begin{aligned}
\mathrm{losses}(\boldsymbol{i}) &= \boldsymbol{i} \cdot \boldsymbol{i} + (i_a + i_b + i_c)^2 = \boldsymbol{i} \cdot \boldsymbol{i} + (\boldsymbol{i} \cdot \boldsymbol{n})^2 \\
&= \mathrm{los}_{\mathrm{norm}} + \mathrm{los}_{\mathrm{sum}},
\end{aligned} \tag{7}$$

where the losses $\boldsymbol{i} \cdot \boldsymbol{i}$ we will call $\mathrm{los}_{\mathrm{norm}}$, the other one $(\boldsymbol{i} \cdot \boldsymbol{n})^2$ we will denote $\mathrm{los}_{\mathrm{sum}}$, and $\boldsymbol{n} = e_1 + e_2 + e_3$.

4.1 PGA realisation

Because we can interpret Eq. (6) as a plane in $\mathbb{R}^3$, we are looking for a solution lying on a particular plane. So, we represent this problem in algebra PGA, i.e., the current will be

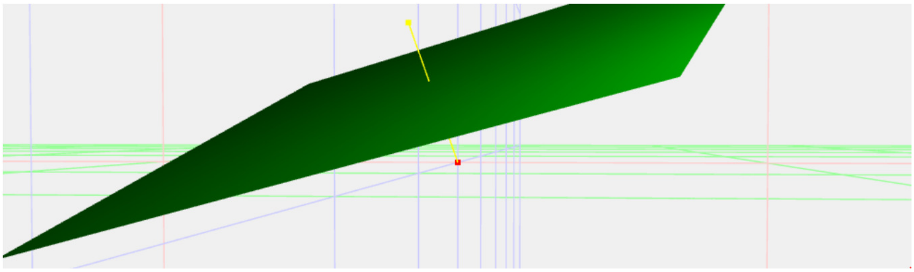

Figure 3. The feasible solution lie on the plane τ.

represented as a PGA point

$$I = (\boldsymbol{i} + e_0)^*,$$

where symbol * stands for PGA duality. Now, points I, which are feasible, that means they satisfy relation (6), lie in the plane τ:

$$\tau = \boldsymbol{v} + pe_0.$$

In Fig. 3, we see the green plane τ, red origin, and a yellow vector $\boldsymbol{v}$ (perpendicular to τ). The important information is the distance of τ from the origin, which codes the power p. Our goal is to minimize the function $\mathrm{losses}(\boldsymbol{i})$ (7). The problem is that part $\mathrm{los}_{\mathrm{norm}}(\boldsymbol{i})$ of the function $\mathrm{losses}(\boldsymbol{i})$ is linear, whereas $\mathrm{los}_{\mathrm{sum}}(\boldsymbol{i})$ is quadratic. In the next section, we will show how to linearize the whole problem by adding a dimension.

4.2 Linearization of the problem

To linearize the quadratic part $\mathrm{los}_{\mathrm{sum}}(\boldsymbol{i})$ and so the function $\mathrm{losses}(\boldsymbol{i})$ (7), we have to extend the workspace by one additional dimension. We use 4D version of PGA, so we add one more Euclidean dimension e_4 to code the sum of coordinates. Now the points, which represent currents in the form

$$I^{4D} = i_a e_1 + i_b e_2 + i_c e_3 - (i_a + i_b + i_c)e_4 + e_0, \tag{8}$$

lie in the hyperplane

$$\rho_0^{4D} = \boldsymbol{n}^{4D} = e_1 + e_2 + e_3 + e_4, \tag{9}$$

and the projection into the original PGA simply forgets the e_4 coordinate from (8) to receive

$$I^{3D} = i_a e_1 + i_b e_2 + i_c e_3 + e_0.$$

Now the feasible solutions lie again on the hyperplane, which is in PGA represented by object

$$\tau = \boldsymbol{v} + pe_0, \tag{10}$$

where $\boldsymbol{v} = v_a e_1 + v_b e_2 + v_c e_3$.

To satisfy conditions (9) and (10), the point I^{4D} must be lying on the hyperline k^{4D}, which is an intersection of the hyperplanes ρ_0^{4D} and τ, i.e.,

$$k^{4D} = \tau \wedge \rho_0^{4D} = \boldsymbol{v} \wedge \boldsymbol{n}^{4D} + pe_0\boldsymbol{n}^{4D}.$$

The function $\operatorname{losses}(\boldsymbol{i})$ is now in the form

$$\operatorname{losses}\bigl(I^{4D}\bigr) = \operatorname{losses}\bigl(\boldsymbol{i}^{4D}\bigr) = I^{4D} \cdot I^{4D},$$

and the minimum is the nearest point to the origin from k. We get this point simply by the projection of the origin e_{1234} to the hyperline k^{4D}, i.e.,

$$I^{4D} = \bigl(k^{4D} \cdot e_{1234}\bigr) \wedge k^{4D}.$$

In coordinates, the previous geometric considerations are represented by the following theorem.

Theorem 1. *Let $\boldsymbol{v} = v_a e_1 + v_b e_2 + v_c e_3 \in \mathbb{R}^3$ be a voltage and $p \in \mathbb{R}$ be a power of the three-phase system. Then the current*

$$\boldsymbol{i} = p\frac{(3v_a - v_b - v_c)e_1 + (3v_b - v_a - v_c)e_2 + (3v_c - v_a - v_b)e_3}{3(v_a^2 + v_b^2 + v_c^2) - 2(v_a v_b + v_b v_c + v_a v_c)} \in \mathbb{R}^3 \tag{11}$$

satisfies the property $\boldsymbol{v} \cdot \boldsymbol{i} = p$, and the $\operatorname{losses}(\boldsymbol{i})$ *is minimal.*

Proof. We represent the current $\boldsymbol{i}$ as a point I^{4D} in 4D PGA and compute the hyperline k^{4D} as follows:

$$\begin{aligned} k^{4D} &= (\boldsymbol{v} + pe_0) \wedge \boldsymbol{n}^{4D} = (v_a e_1 + v_b e_2 + v_c e_3) \wedge \boldsymbol{n}^{4D} - p\boldsymbol{n}^{4D} e_0 \\ &= (v_b - v_c)e_{23} + (v_c - v_a)e_{31} + (v_a - v_b)e_{12} \\ &\quad + v_a e_{14} + v_b e_{24} + v_c e_{34} - p\boldsymbol{n}^{4D} e_0. \end{aligned}$$

The hyperline l^{4D} perpendicular to the hyperline k^{4D} can be obtained by the inner product as

$$\begin{aligned} l^{4D} &= k^{4D} \cdot e_{1234} \\ &= (v_b - v_c)e_{14} + (v_c - v_a)e_{24} + (v_a - v_b)e_{34} + v_a e_{23} + v_b e_{13} + v_c e_{12}, \end{aligned}$$

and the intersection of the hyperline l^{4D} and the hyperline k^{4D} is then the projection of the origin to the hyperline k^{4D}, and therefore the final point

$$\begin{aligned} I^{4D} &= l^{4D} \wedge k^{4D} \\ &= p(3v_a - v_b - v_c)e_{2340} + p(3v_b - v_a - v_c)e_{3140} + p(3v_c - v_a - v_b)e_{1240} \\ &\quad + \bigl(3\bigl(v_a^2 + v_b^2 + v_c^2\bigr) - 2(v_a v_b + v_b v_c + v_a v_c)\bigr)e_{1234} + \alpha e_{0123}, \end{aligned}$$

where α is a real number, but the blade $e_{0123}^* = e_4$ is forgotten by the projection in to 3D. Finally, after homogenization and projection, we received

$$I^{3D} = \boldsymbol{i} + e_0,$$

where

$$\boldsymbol{i} = p\frac{(3v_a - v_b - v_c)e_1 + (3v_b - v_a - v_c)e_2 + (3v_c - v_a - v_b)e_3}{3(v_a^2 + v_b^2 + v_c^2) - 2(v_a v_b + v_b v_c + v_a v_c)},$$

which completes the proof. □

Corollary 2. *The current from* (11) *can also be expressed with the help of the inner product as*

$$\boldsymbol{i} = p\frac{4\boldsymbol{v} - (v_a + v_b + v_c)\boldsymbol{n}}{4(\boldsymbol{v}\cdot\boldsymbol{v}) - (v_a + v_b + v_c)^2}.$$

Proof. The straightforward computation

$$\begin{aligned}
\boldsymbol{i} &= p\frac{(3v_a - v_b - v_c)e_1 + (3v_b - v_a - v_c)e_2 + (3v_c - v_a - v_b)e_3}{4(\boldsymbol{v}\cdot\boldsymbol{v}) - (v_a + v_b + v_c)^2} \\
&= p\frac{4\boldsymbol{v} - (v_a + v_b + v_c)\boldsymbol{n}}{3(v_a^2 + v_b^2 + v_c^2) - 2(v_a v_b + v_b v_c + v_a v_c)} = p\frac{4\boldsymbol{v} - (v_a + v_b + v_c)\boldsymbol{n}}{4(\boldsymbol{v}\cdot\boldsymbol{v}) - (v_a + v_b + v_c)^2} \\
&= p\frac{4\boldsymbol{v} - (\boldsymbol{v}\cdot\boldsymbol{n})\boldsymbol{n}}{4(\boldsymbol{v}\cdot\boldsymbol{v}) - (\boldsymbol{v}\cdot\boldsymbol{n})^2}
\end{aligned}$$

completes the proof. □

Corollary 3. *If system* (5) *is symmetric, so* $v_a + v_b + v_c = 0$*, then the current from* (11) *can be expressed in the form*

$$\boldsymbol{i} = p\frac{\boldsymbol{v}}{(\boldsymbol{v}\cdot\boldsymbol{v})}.$$

The following theorem explains how the minimum losses for the observed current can by computed.

Theorem 2. *Let* $\boldsymbol{v} = v_a e_1 + v_b e_2 + v_c e_3 \in \mathbb{R}^3$ *be a voltage,* $p \in \mathbb{R}$ *be a power of the three-phase system, and current* $\boldsymbol{i}$ *be a current* (11) *from Theorem* 1*. Then the losses function from* (7) *is in the following form*:

$$\operatorname{losses}(\boldsymbol{i}) = \frac{4p^2}{4\|\boldsymbol{v}\|^2 - (v_a + v_b + v_c)^2}.$$

Proof. For current from Theorem 1, we have

$$\begin{aligned}
\boldsymbol{i} &= \alpha\big(4\boldsymbol{v} - (v_a + v_b + v_c)\boldsymbol{n}\big) \\
&= \alpha\big(4(v_a e_1 + v_b e_2 + v_c e_3) - (v_a + v_b + v_c)(e_1 + e_2 + e_3)\big) \\
&= \alpha\big((3v_a - v_b - v_c)e_1 + (3v_b - v_a - v_c)e_2 + (3v_c - v_a - v_b)e_3\big) \\
\boldsymbol{i}\cdot\boldsymbol{i} &= \alpha^2\big((3v_a - v_b - v_c)^2 + (3v_b - v_a - v_c)^2 + (3v_c - v_a - v_b)^2\big) \\
&= \alpha^2\big(11\big(v_a^2 + v_b^2 + v_c^2\big) - 10(v_a v_b + v_b v_c + v_a v_c)\big),
\end{aligned}$$

$$\begin{aligned}(i_a + i_b + i_c)^2 &= \alpha^2 (v_a + v_b + v_c)^2 \\ &= \alpha^2 \bigl(v_a^2 + v_b^2 + v_c^2 + 2(v_a v_b + v_b v_c + v_a v_c)\bigr),\end{aligned}$$

where $\alpha = p/(4(\boldsymbol{v} \cdot \boldsymbol{v}) - (v_a + v_b + v_c)^2)$. Finally, because of

$$\begin{aligned}\boldsymbol{i} \cdot \boldsymbol{i} + (i_a + i_b + i_c)^2 &= 4\alpha^2 \bigl(3\bigl(v_a^2 + v_b^2 + v_c^2\bigr) - 2(v_a v_b + v_b v_c + v_a v_c)\bigr) \\ 4(\boldsymbol{v} \cdot \boldsymbol{v}) - (v_a + v_b + v_c)^2 &= 3\bigl(v_a^2 + v_b^2 + v_c^2\bigr) - 2(v_a v_b + v_b v_c + v_a v_c),\end{aligned}$$

we have

$$\text{losses}(\boldsymbol{i}) = \frac{4p^2(3(v_a^2 + v_b^2 + v_c^2) - 2(v_a v_b + v_b v_c + v_a v_c))}{(3(v_a^2 + v_b^2 + v_c^2) - 2(v_a v_b + v_b v_c + v_a v_c))^2} = 4p\alpha,$$

which completes the proof. □

Example 1. We demonstrate our algorithm on the same example as in the paper [14], then we have

$$\boldsymbol{v} = -3e_1 + 9e_2 - 2e_3, \qquad \boldsymbol{i}_{\text{orig}} = -9e_1 + 2e_2 - 5e_3,$$

so the electric power is

$$p = \boldsymbol{v} \cdot \boldsymbol{i}_{\text{orig}} = 55.$$

Now we can use formula (11) from Theorem 1

$$\begin{aligned}\boldsymbol{i} &= 55 \frac{(-9 - 9 + 2)e_1 + (27 + 3 + 2)e_2 + (-6 + 3 - 9)e_3}{3((-3)^2 + 9^2 + (-2)^2) - 2(-27 - 18 + 6)} \\ &= 55 \frac{-16e_1 + 32e_2 + -12e_3}{3(94) - 2(-39)} = 55 \frac{-16e_1 + 32e_2 + -12e_3}{360} \\ &= \frac{-44e_1 + 88e_2 + -33e_3}{18} = -2.44e_1 + 4.89e_2 - 1.83e_3,\end{aligned}$$

and we get the same result as in the paper [14], where the losses are

$$\text{losses}(\boldsymbol{i}) = \frac{4 \cdot 55^2}{4(9 + 81 + 4) - 16} = 33,6\overline{1}.$$

4.3 Compensation

By compensation we mean a transformation that optimally converts the original current I_{orig} to the calculated current I. We will discuss compensation in the following sections with respect to time t. Here we note that if the system were not time-dependent, the optimal trajectory would be a line segment, and the compensation would be translation

$$\mathcal{T} = 1 - 0.5(\boldsymbol{i} - \boldsymbol{i}_{\text{orig}})e_0.$$

In this case, the trajectory is still in hyperplane τ.

5 Symmetric three phase voltage supply

In this section, we will consider the situation where harmonic three-phase voltage and current inputs are in the form without offset, i.e.,

$$V = v_a(t)e_1 + v_b(t)e_2 + v_c(t)e_3,$$
$$I = i_a(t)e_1 + i_b(t)e_2 + i_c(t)e_3,$$

where $v_s(t)$ and $i_s(t)$, $s \in \{a, b, c\}$, are from (5), i.e., $V_n = I_n = 0$. In this case, we will see that a current is in the same plane as a voltage. The given current I_{orig} and voltage V are moving on concentric circles with a radius depending on amplitude $I_{\max}$ and $V_{\max}$, and a current is shifted by φ. These facts follow directly from formulas (5).

Note that according to Lemma (2), we can represent the three-phase systems (5) as an orbits with respect to rotation in the plane $\rho_0 = e_1 + e_2 + e_3$, i.e.,

$$\mathcal{R}_{\boldsymbol{v}}(t) = \exp\left(-\frac{1}{2}\omega t \frac{e_{23} + e_{31} + e_{12}}{\sqrt{3}}\right), \quad \text{where } t \in \langle 0, \infty).$$

So, the plane $\tau(t) = \boldsymbol{v}(t) + 3V_{\max}I_{\max}\cos(\varphi)e_0$ depends on the time t, and the optimal current $I(t)$ is the projection of origin onto the plane τ. The value of a current $I(t)$ rotates on the circle with radius $\sqrt{3}I_{\max}\cos(\varphi)$.

Example 2. In Fig. 4, we see the trajectories of currents $I_{\mathrm{orig}}(t)$, $I(t)$ and voltage $V(t)$ for

$$I_{\max} = 0.7, \quad V_{\max} = 1.2, \quad \varphi = 0.2\pi.$$

In the time $t_0 = 0$, the given voltage $V(t_0)$ as point $A[1.2, -0.6, -0.6]$, given current $I_{\mathrm{orig}}(t_0)$ as point $B[0.57, -0.64, 0.07]$, and the optimal current $I(t_0)$ as point $C[0.57, -0.28, -0.28]$ (at time $t = 0$) are represented there.

Transformation from $I_{\mathrm{orig}}(t_0)$ to $I(t_0)$ can be done directly by translation or by rotation and dilation. The direction of translation $I(t) - I_{\mathrm{orig}}(t)$ (the points C–B in

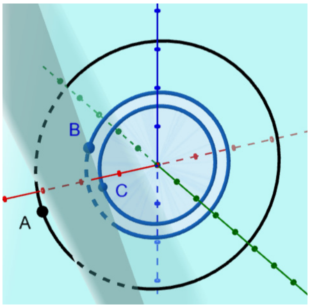

Figure 4. Voltage moves along the outer circle, original current I_{orig} along the middle one, the final current I along the inner one.

Example 2 depends on time and can be represented in PGA by translator

$$\begin{aligned}\mathcal{T}(t) &= \exp\left(-\frac{1}{2}\sin(\varphi)\|\boldsymbol{i}\|\frac{(\boldsymbol{v}(t)\wedge\boldsymbol{n})e_{123}}{\|\boldsymbol{n}\|\|\boldsymbol{v}\|}e_0\right)\\ &= \exp\left(-\frac{1}{2}\sin(\varphi)\sqrt{2}I_{\max}\frac{(\boldsymbol{v}(t)\wedge\boldsymbol{n})e_{123}}{\sqrt{3}V_{\max}}e_0\right)\end{aligned}$$

or in CGA by translator

$$\begin{aligned}\mathcal{T}(t) &= \exp\left(-\frac{1}{2}\sin(\varphi)\|\boldsymbol{i}\|\frac{(\boldsymbol{v}(t)\wedge\boldsymbol{n})e_{123}}{\|\boldsymbol{n}\|\|\boldsymbol{v}\|}e_\infty\right)\\ &= \exp\left(-\frac{1}{2}\sin(\varphi)\sqrt{2}I_{\max}\frac{(\boldsymbol{v}(t)\wedge\boldsymbol{n})e_{123}}{\sqrt{3}V_{\max}}e_\infty\right).\end{aligned}$$

To eliminate the dependence on the time, we use CGA algebra, which may additionally represent dilation with help of versor

$$\mathcal{D} = 1 + \frac{1-d}{1+d}e_{45}.$$

The dilation is constant with proportion (ratio) equal to $|\cos(\varphi)|$, so the versor is

$$\mathcal{D} = 1 + \frac{1-|\cos(\varphi)|}{1+|\cos(\varphi)|}e_{45}.$$

If we rotate I_{orig} in the constant plane ρ_0, then the angle of rotation φ is constant, too. By rotation $\mathcal{R}$ of $I_{\mathrm{orig}}(t)$ we received the vector parallel to the vector $V(t)$, where

$$\mathcal{R} = \cos\frac{\varphi}{2} - \sin\frac{\varphi}{2}\frac{e_{23}+e_{31}+e_{12}}{\sqrt{3}} = \exp\left(-\frac{1}{2}\varphi\frac{e_{23}+e_{31}+e_{12}}{\sqrt{3}}\right).$$

In particular, we need to map circle with radius $I_{\max}\sqrt{1.5}$ of $I_{\mathrm{orig}}(t)$ to circle with radius $|\cos(\varphi)|I_{\max}\sqrt{1.5}$ of $I(t)$. Both circles have a center at the origin. In such a way, we found the transformation $\mathcal{DR}$ from I_{orig} to I, which is not time-dependent, i.e.,

$$I = \mathcal{D}\mathcal{R}I_{\mathrm{orig}}\mathcal{R}^{-1}\mathcal{D}^{-1}.$$

5.1 Bivector corresponding to the dilation

During the generation of Fig. 3, we used the fact that we can represent transformations as exponential of bivectors. If we introduce substitution $d = \mathrm{e}^{-2a}$, where $a = -0.5\ln(d) = -0.5\ln(|\cos(\varphi)|)$, then the dilations can be rewritten as

$$\begin{aligned}\mathcal{D} &= 1 + \frac{1-d}{1+d}e_{45} = 1 + \frac{1-\mathrm{e}^{-2a}}{1+\mathrm{e}^{-2a}}e_{45} = 1 + \frac{\mathrm{e}^{a}-\mathrm{e}^{-a}}{\mathrm{e}^{a}+\mathrm{e}^{-a}}e_{45}\\ &= 1 + \tanh(a)e_{45}.\end{aligned}$$

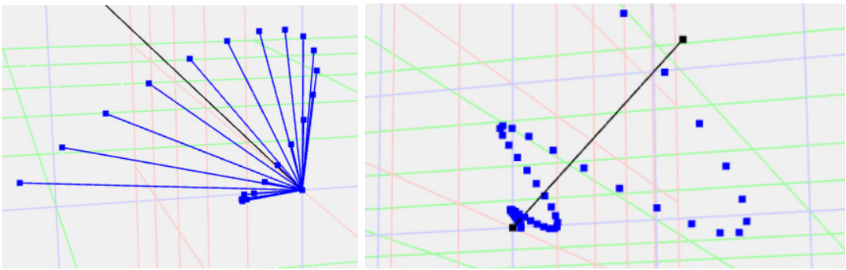

Figure 5. Compensation based on rotation and dilation.

On the other hand, the Taylor expansion of function $\exp$ can be rewritten as

$$\exp(ae_{45}) = \sum_{n=0}^{\infty} \frac{a^{2n}}{(2n)!} + \sum_{n=0}^{\infty} \frac{a^{2n+1}}{(2n+1)!} e_{45} = \cosh a + \sinh a e_{45}$$

because of $e_{45}^2 = 1$. So we can get

$$\cosh(a)\bigl(1 + \tanh(a)e_{45}\bigr) = \exp(ae_{45}) = \exp\bigl(-0.5 \ln\bigl(\bigl|\cos(\varphi)\bigr|\bigr)e_{45}\bigr),$$

and finally, we can see that

$$\mathcal{D} = \exp\bigl(-0.5 \ln\bigl(\bigl|\cos(\varphi)\bigr|\bigr)e_{45}\bigr)$$

after the expression is divided by $\cosh(d)$. Finally, note that composition of rotation and dilation leads to

$$\begin{aligned}\mathcal{RD} &= \exp\left(\varphi \frac{e_{23} + e_{31} + e_{12}}{2\sqrt{3}}\right) \exp\bigl(-0.5 \ln\bigl(\bigl|\cos(\varphi)\bigr|\bigr)e_{45}\bigr) \\ &= \exp\left(\varphi \frac{e_{23} + e_{31} + e_{12}}{2\sqrt{3}} - 0.5 \ln\bigl(\bigl|\cos(\varphi)\bigr|\bigr)e_{45}\right),\end{aligned}$$

where these equations hold for angles $|\varphi| < \pi/2$.

6 Voltage supply with DC offset

In the more general case, we deal with three-phase power systems with DC offset. In Section 5, the voltage and current lie in plane $\rho_0 = \boldsymbol{n}$. In a more general case (4), the situation is not that simple, but still we know that current and voltage lie on planes parallel to ρ_0. In this case, the circle's center must be a projection of the origin onto the plane for the power to be constant in time. So we suppose they lie on circles, and their rotation has the same frequency.

Theorem 3. *In three phased power system based on Eqs.* (4)*, the optimal currency can be represented by a circle*

$$\boldsymbol{i}(t) = \frac{V_n I_n + V_{\max} I_{\max} \cos(\varphi)}{V_n^2 + 4V_{\max}^2} \bigl(4\boldsymbol{v}(t) - 3V_n \boldsymbol{n}\bigr) \tag{12}$$

with center

$$\frac{V_n I_n + V_{\max} I_{\max} \cos(\varphi)}{V_n^2 + 4V_{\max}^2} \boldsymbol{n} V_n$$

and radius

$$\sqrt{3} \frac{V_n I_n + V_{\max} I_{\max} \cos(\varphi)}{V_n^2 + 4V_{\max}^2} 4V_{\max}.$$

Proof. We will compute the current $\boldsymbol{i}$ from Theorem 1 in the form

$$\boldsymbol{i} = p \frac{4\boldsymbol{v} - (v_a + v_b + v_c)\boldsymbol{n}}{4(\boldsymbol{v} \cdot \boldsymbol{v}) - (v_a + v_b + v_c)^2}. \tag{13}$$

The sum $v_a + v_b + v_c$ of voltages from (4) is directly equal to $3V_n$ because the period between phases is $2\pi/3$. So the numerator of (13) gives us the direction $4\boldsymbol{v} - 3V_n\boldsymbol{n}$. The denominator of (13) can by directly computed as

$$12\bigl(V_n^2 + V_{\max}^2\bigr) - (3V_n)^2 = 12V_n^2 + 3V_{\max}^2,$$

and the power p is based on lemma 1, which completes the proof. $\square$

Corollary 4. *Let* $\boldsymbol{v} = v_a e_1 + v_b e_2 + v_c e_3 \in \mathbb{R}^3$ *be a voltage based on system* (4)*,* $p \in \mathbb{R}$ *be a power of the three-phase system, and the current* $\boldsymbol{i}$ *be a current* (12) *from Theorem* 3*. Then the losses function from* (7) *is in the following form*:

$$\text{losses}(\boldsymbol{i}) = \frac{4p^2}{4\|\boldsymbol{v}\|^2 - 9V_n^2}.$$

We are seeking a transformation from the original current circle, i.e., circle with the center $\boldsymbol{n}I_n$ and radius $\sqrt{3}I_{\max}$, to the optimal one from Theorem 3.

Theorem 4. *The dilation that maps the original current circle* (4) *to the current circle based on* (12) *based on a ratio*

$$d = \frac{4V_{\max}}{I_{\max}} \frac{V_n I_n + V_{\max} I_{\max} \cos(\varphi)}{V_n^2 + 4V_{\max}^2}$$

with the center

$$\boldsymbol{c} = \boldsymbol{n} \frac{4V_{\max} I_n - V_n I_{\max}}{4V_{\max} - I_{\max} \frac{V_n^2 + 2V_{\max}^2}{V_n I_n + V_{\max} I_{\max} cos(\varphi)/2}}.$$

Proof. Both circles lie on the cone with the top $\boldsymbol{c}$, and the ratio for dilation should be the ratio of the radii

$$d = \frac{4\frac{V_n I_n + V_{\max} I_{\max} \frac{1}{2}\cos(\varphi)}{V_n^2 + 2V_{\max}^2}\sqrt{\frac{3}{2}}V_{\max}}{\sqrt{\frac{3}{2}}I_{\max}} = \frac{4V_{\max}}{I_{\max}}\frac{V_n I_n + V_{\max} I_{\max}\frac{1}{2}\cos(\varphi)}{V_n^2 + 2V_{\max}^2},$$

which completes the proof. □

Corollary 5. *In general, three-phase power system from* (4) *has an optimal currency*

$$\operatorname{losses}(\boldsymbol{i}) = \frac{4p^2}{3V_n^2 + 6V_{\max}^2}.$$

Proof. Straightforward calculation

$$\begin{aligned}\operatorname{losses}(\boldsymbol{i}) &= \frac{4p^2}{4\|\boldsymbol{v}\|^2 - (v_a + v_b + v_c)^2} = \frac{4p^2}{12V_n^2 + 12V_{\max}^2 - 9V_n^2} \\ &= \frac{4p^2}{3V_n^2 + 12V_{\max}^2}\end{aligned}$$

completes the proof. □

Our aim is to map a circle with the centre $\boldsymbol{s}_1 = \boldsymbol{n}I_n$ and the radius $r_1 = \sqrt{3}I_{\max}$ into a circle with the following centre $\boldsymbol{s}_2$ and radius r_2:

$$\boldsymbol{s}_2 = \frac{V_n I_n + V_{\max} I_{\max}\cos(\varphi)}{V_n^2 + 4V_{\max}^2}\boldsymbol{n}V_n, \qquad r_2 = \sqrt{3}\frac{V_n I_n + V_{\max} I_{\max}\cos(\varphi)}{V_n^2 + 4V_{\max}^2}4V_{\max}.$$

From Theorem 4 we know ratio $d = r_2/r_1$, and we can find the dilation with the center in origin:

$$\mathcal{D} = \exp\biggl(-\frac{1}{2}\ln\bigl(|d|\bigr)e_{45}\biggr).$$

This transformation gives us a circle of the correct radius. We still need to solve for the position. The translation in the direction of $\boldsymbol{n}$ by

$$\mathcal{T} = \exp\biggl(-\frac{1}{2}\boldsymbol{s}e_\infty\biggr),$$

where $\boldsymbol{s} = \boldsymbol{s}_2 - d\boldsymbol{s}_1$, places the first circle on the second. Finally, rotate by an angle $-\varphi$ around $\boldsymbol{n}$ as in the previous section. Overall, the transformation is independent of time, i.e.,

$$I = \mathcal{RTD}I_{\text{orig}}\mathcal{D}^{-1}\mathcal{T}^{-1}\mathcal{R}^{-1}.$$

The resulting motions could be characterized as a helix on a cone and are displayed in Fig. 5, and the mentioned circles can bee seen in Fig. 6.

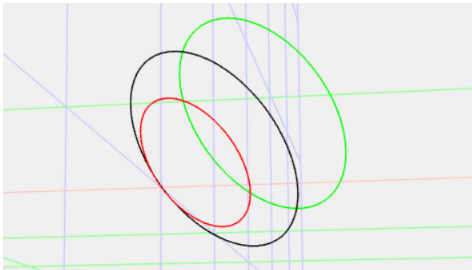

Figure 6. Original circle (red), circle after dilation (black), final circle (green).

7 Conclusion

In a fix time t_0, we find the current $\boldsymbol{i}$ for which the system has minimal losses due to additional constraints. It holds for any power system (balanced, unbalanced, with or without offset). This result is formalized in Theorem 1. Note that the current found in this way lies on a parallel plane and a common cone.

For a symmetric system with or without DC offset, we find a conformal transformation that converts $\boldsymbol{i}_{\mathrm{orig}}$ to $\boldsymbol{i}$ so that the trajectories of the transformation are optimal, and the mentioned transformation is time-depending. This result is formalized in Theorem 4.

We showed that using the mathematical apparatus of geometric algebras allows us to find a suitable transformation efficiently.

Author contributions. The authors (J.B. and J.H.) have contributed as follows: writing – original draft, investigation, J.B.; conceptualization, methodology, J.H. All authors have read and approved the published version of the manuscript.

Conflicts of interest. The authors declare no conflicts of interest.

Acknowledgment. We want to thank Paco for his valuable comments and support.

References

1. S. Breuils, K. Tachibana, E. Hitzer, New applications of Clifford's geometric algebra, *Adv. Appl. Clifford Algebras*, **32**:17, 2022, `https://doi.org/10.1007/s00006-021-01196-7`.

2. F. Casado-Machado, J.L. Martínez-Ramos, M. Barragán-Villarejo, J.M. Maza-Ortega, Reduced reference frame transformation assessment in unbalanced three-phase four-wire systems, *IEEE Access*, **11**:24591–24603, 2023, `https://doi.org/10.1109/ACCESS.2023.3254299`.

3. L. Dorst, S. De Keninck, A Guided Tour to the Plane-Based Geometric Algebra (PGA), `https://bivector.net/PGA4CS.pdf`.

4. L. Dorst, D. Fontijne, S. Mann, *Geometric Algebra for Computer Science: An Object-Oriented Approach to Geometry*, Morgan Kaufm. Ser. Comput. Graph., Elsevier, Amsterdam, 2007.

5. A.H. Eid, F.G. Montoya, A systematic and comprehensive geometric framework for multiphase power systems analysis and computing in time domain, *IEEE Access*, **10**:132725–132741, 2022, https://doi.org/10.1109/ACCESS.2022.3230915.
6. D. Hildenbrand, *Foundations of Geometric Algebra Computing*, Geom. Comput., Springer, Berlin, Heidelberg, 2012, https://doi.org/10.1007/978-3-642-31794-1.
7. D. Hildenbrand, J. Hrdina, A. Návrat, P. Vašík, Local controllability of snake robots based on CRA, theory and practice, *Adv. Appl. Clifford Algebras*, **30**:2, 2020, https://doi.org/10.1007/s00006-019-1022-8.
8. E. Hitzer, M. Kamarianakis, G. Papagiannakis, P. Vašík, Survey of new applications of geometric algebra, *Math. Methods Appl. Sci.*, **47**(14):11368–11384, 2024, https://doi.org/10.1002/mma.9575.
9. E. Hitzer, C. Lavor, D. Hildenbrand, Current survey of Clifford geometric algebra applications, *Math. Methods Appl. Sci.*, **47**(3):1331–1361, 2022, https://doi.org/10.1002/mma.8316.
10. J. Hrdina, A. Návrat, Binocular computer vision based on conformal geometric algebra, *Adv. Appl. Clifford Algebras*, **27**(3):1945–1959, 2017, https://doi.org/10.1007/s00006-017-0764-4.
11. J. Hrdina, A. Návrat, P. Vašík, Notes on planar inverse kinematics based on geometric algebra, *Adv. Appl. Clifford Algebras*, **28**(3):71, 2018, https://doi.org/10.1007/s00006-018-0890-7.
12. J. Hrdina, A. Návrat, P. Vašík, L. Dorst, Projective geometric algebra as a subalgebra of conformal geometric algebra, *Adv. Appl. Clifford Algebras*, **31**(2):18, 2020, https://doi.org/10.1007/s00006-021-01118-7.
13. P. Lounesto, *Clifford Algebras and Spinors*, Cambridge Handbooks for Language Teachers, Cambridge Univ. Press, 2001, https://doi.org/10.1017/CBO9780511526022.
14. F.G. Montoya, A.H. Eid, Formulating the geometric foundation of Clarke, Park, and FBD transformations by means of Clifford's geometric algebra, *Math. Methods Appl. Sci.*, **45**(8): 4252–4277, 2021, https://doi.org/10.1002/mma.8038.
15. F.G. Montoya, X. Prado, F.M. Arrabal-Campos, A. Alcayde, J. Mira, New mathematical model based on geometric algebra for physical power flow in theoretical two-dimensional multi-phase power circuits, *Sci. Rep.*, **13**:1128, 2023, https://doi.org/10.1038/s41598-023-28052-x.
16. C. Perwass, *Geometric Algebra with Applications in Engineering*, Geom. Comput., Springer, Berlin, Heidelberg, 2009, https://doi.org/10.1007/978-3-540-89068-3.
17. J. Ventura, F. Martínez, F. Manzano-Agugliaro, A. Návrat, J. Hrdina, A.H. Eid, F.G. Montoya, A novel geometric method based on conformal geometric algebra applied to the resection problem in two and three dimensions, *J. Geod.*, **98**:47, 2024, https://doi.org/10.1007/s00190-024-01854-1.
18. E. Viciana, F.M. Arrabal-Campos, A. Alcayde, R. Baños, F.G. Montoya, All-in-one three-phase smart meter and power quality analyzer with extended IoT capabilities, *Measurement*, **206**: 112309, 2023, https://doi.org/10.1016/j.measurement.2022.112309.